Journal of Solid State Chemistry 182 (2009) 1273–1280

Contents lists available at ScienceDirect

Journal of Solid State Chemistry

journal homepage: www.elsevier.com/locate/jssc

# Improvement by heating of the electronic conductivity of cobalt spinel phases, electrochemically synthesized in various electrolytes

Myriam Douin [a,b,c], Liliane Guerlou-Demourgues [a,b,*], Michel Ménétrier [a,b], Emilie Bekaert [a,b], Lionel Goubault [c], Patrick Bernard [c], Claude Delmas [a,b]

[a] CNRS, ICMCB, 87, Av. Dr. A. Schweitzer, 33608 Pessac Cedex, France
[b] Université de Bordeaux, ICMCB, ENSCPB, F33608 Pessac Cedex, France
[c] SAFT - Direction de la Recherche 111-113 Boulevard Alfred Daney, 33074 Bordeaux Cedex, France

ARTICLE INFO

*Article history:*
Received 18 July 2008
Received in revised form
9 February 2009
Accepted 10 February 2009
Available online 21 February 2009

*Keywords:*
Spinel
Cobalt oxide
Electronic conductivity
Alkaline battery

ABSTRACT

The nature of the alkaline electrolyte (based on KOH, NaOH, LiOH), in which $Co_3O_4$ spinel type phases are synthesized by electrooxidation of CoO, is shown to play a key role on the composition, the structure and the electronic conductivity of the materials. In the materials, prepared in pure LiOH electrolyte or in mixed ternary electrolyte (KOH, NaOH, LiOH), $Co^{4+}$ ions are present in the octahedral framework, which entails electronic delocalization in the cobalt $T_{2g}$ band and a high conductivity. The structure of the sample, synthesized in KOH, is on the opposite closer to that of ideal $Co_3O_4$, with only $Co^{3+}$ in the octahedral sublattice, which leads to a semi-conducting behavior. Whatever the initial material, a thermal treatment induces an increase of the $Co^{4+}/Co^{3+}$ ratio in the octahedral network, resulting in a significant increase of the electronic conductivity.



## 1. Introduction

Because of the poor electronic conductivity of nickel hydroxide, which is the electroactive material at the nickel oxide electrode (NOE) positive electrode of alkaline batteries, the role of the conductive additive is crucial. Usually, a conductive network is formed during the first charge of the battery from CoO or $Co(OH)_2$ phases, which are added to nickel hydroxide particles during the electrode manufacturing [1,2]. The conductive properties of this network result from the oxidation of the added cobalt phases into non stoichiometric $H_xCoO_2$ type phases, in which the presence of tetravalent cobalt allows to reach a good conductivity [3,4]. In modern nickel–metal hydride batteries, which are now especially developed for high power applications, the occurrence of deep discharges tends to damage the conductive network, by reducing the conductive oxyhydroxide phases into cobalt hydroxide, which is partly dissolved in the electrolyte [5,6]. Many works have been reported in the literature, aiming at stabilizing this conductive network [5–9].

An industrial process consists in performing the first charge of Ni–MH and Ni–Cd cells in very specific conditions, to optimize the conductive cobalt network within the electrode [10,11]. Previous works performed have shown that conductive $Co_3O_4$ type phases are obtained in such conditions, and constitute a high-performance network. Such phases contain cobalt vacancies in both tetrahedral and octahedral sites, as well as lithium (coming from the electrolyte) and hydrogen in the structure. The lack of positive charge due to cobalt vacancies is not fully compensated by lithium and protons, leading to the formation of tetravalent cobalt in octahedral sites. As a result of the electronic configuration of $Co^{4+}$ ($d^5$), electronic delocalization occurs in the octahedral sublattice, through an overlapping of the $t_{2g}$ cobalt orbitals. Such behavior entails good electronic conduction properties, with a p-type metallic conductivity [12].

The effect of heat treatment on the conductivity of such cobalt spinel phases, synthesized in a mixed KOH–LiOH–NaOH electrolyte, was investigated very recently in our laboratory, through, in particular, an XRD analysis coupled with thermal treatment. The material exhibits simultaneously, around 350 °C, a significant increase in electronic conductivity, a departure of $H_2O$, as well as an increase of the Co/O atomic ratio and of the amount of $Co^{2+}$ in tetrahedral sites. On the basis of these results, the evolution of the material has been explained by an increase in the $Co^{4+}/Co^{3+}$ atomic ratio in the octahedral framework, which leads to an increase of electronic conductivity by 3 orders of magnitude [13].

The chemical composition of the starting spinel phase is strongly depending on the nature of the electrolyte, used for the electrochemical synthesis [12]. Therefore, the evolution of the structure and of the electronic properties of the spinel phases, during a thermal treatment, will be studied and discussed, in the

* Corresponding author. Fax: +33 540006698.
*E-mail address:* guerlou@icmcb-bordeaux.cnrs.fr (L. Guerlou-Demourgues).

0022-4596/$ - see front matter © 2009 Elsevier Inc. All rights reserved.
doi:10.1016/j.jssc.2009.02.018

present paper, as a function of the electrolyte nature: pure KOH, pure LiOH or ternary electrolyte (LiOH–NaOH–KOH). The results concerning the latter electrolyte were published elsewhere [13] and will be used for comparison purpose.

## 2. Experimental

### 2.1. Material preparation

Materials were synthesized by electrochemical oxidation of a cobalt-based electrode. The electrode was made from a viscous paste, prepared by mixing CoO powder with 50 wt% deionised water. The electrode was placed between two cadmium electrodes, playing both roles of counter and reference electrode. The cell was first left during 4 days in the electrolyte, to allow complete hydrolysis of CoO into $Co(OH)_2$. In the so-constituted cell, the CoO-based electrode was the positive pole and the Cd-based electrode the negative one. Therefore, charge and discharge of the cell correspond to cobalt oxidation and reduction, respectively. Usual electrolyte is a ternary concentrated alkaline electrolyte, consisting of NaOH, LiOH and majority KOH. In order to study the influence of alkaline ions of electrolyte, two other media were used: 8 M-KOH and saturated LiOH solution. Oxidation was performed during 120 h, at the $C/100$ rate, in KOH and ternary electrolyte, and during 60 h, at $C/40$, in LiOH electrolyte. (The theoretical capacity "$C$" of the battery was calculated on the basis of one electron exchanged per cobalt atom). In the following, the so obtained materials will be denoted as $Co_3O_4$(KOH), $Co_3O_4$ (LiOH), $Co_3O_4$(ternary), depending on the electrolyte used for synthesis.

### 2.2. Characterization

X-ray diffraction (XRD) data were collected with a PANalytical X'pert Pro diffractometer using the Co$K\alpha$ radiation. The diffraction patterns were recorded in the [5°–110°] ($2\theta$) angular range, using a 0.0167° ($2\theta$) step, with an active width of 2.122° in the detector and a constant counting time of 250 s/step.

The effect of heat-treatment on the structure of the materials, prepared in the various electrolytes, was followed in-situ by XRD, thanks to a variable temperature chamber (Anton Paar HTK 1200 high temperature furnace), connected to the diffractometer. These experiments allow to obtain more insight on the composition of the materials. The sample was heated at the rate of 3 °C/min, and isothermal stages of four hours were performed every 100 °C, from RT to 700 °C, and every 200 °C, from 700 °C to RT, during which the XRD data were collected.

Structure refinements were based on the Rietveld method, using the Fullprof program. The diffraction peaks were described by pseudo-Voigt fitting function, in which the Lorentzian contribution to the Gaussian peak-shape was refined. The angular dependence of the widths was expressed by $H^2 = U\tan^2\theta + V\tan\theta + W$, where $H$ is the full-width at half-maximum, $\theta$ is the Bragg angle and, $U$, $V$ and $W$ are refined parameters. Due to the Co radiation, the anomalous scattering factors were added as below $f'(\mathrm{Li}) = 0.0130$, $f''(\mathrm{Li}) = 0.0005$, $f'(\mathrm{O}) = 0.0630$, $f''(\mathrm{O}) = 0.0440$, $f'(\mathrm{Co}) = -2.0230$ and $f''(\mathrm{Co}) = 0.5731$. Background intensities were fixed with about 20 experimental points. The spinel-type phase was described in the cubic space group $Fd_3/m$, with oxygen in 32$e$ positions ($u$,$u$,$u$) and with cobalt ions located in the 8$a$ tetrahedral sites ($\frac{1}{8},\frac{1}{8},\frac{1}{8}$) and in the 16$d$ octahedral sites ($\frac{1}{2},\frac{1}{2},\frac{1}{2}$). Scale factor, lattice parameter, atomic position of oxygen, cobalt occupancy, and thermal displacement parameters $B$ were refined. CoOOH and $LiCoO_2$ type phases were described in the space group $R3m$, with oxygen atoms in 6$c$ positions (0,0,$z$), cobalt ions in 3$a$ sites (0,0,0) and lithium ions (for $LiCoO_2$ phase only) in 3$b$ sites $(0,0,\frac{1}{2})$. CdO type phase was described in the cubic space group $Fm_3/m$, with cadmium atoms in 4$a$ sites (0,0,0) and oxygen atoms in 4$b$ sites $(\frac{1}{2},\frac{1}{2},\frac{1}{2})$. For these secondary phases, present in small quantities (less than 10 wt%), only scale factor, lattice parameter and atomic position were refined.

Inductively coupled plasma (ICP) was used for Li, Na, K and Co titration, and elementary organic microanalysis was used for H titration; titrations were performed at CNRS facility in Vernaison (France). The oxidation state of cobalt was determined by iodometric titration method [12].

Thermogravimetric analysis (TGA) was carried out with a TA Instruments SDT 600 analyzer, under an oxygen flux, from room temperature to 1000 °C, at a heating rate of 1 °C/min.

$^7$Li MAS NMR spectra were recorded on a Bruker Avance 300 (116.6 MHz) spectrometer, using a standard 2.5 mm Bruker MAS probe, with a 30 kHz spinning speed. A simple pulse sequence was used, with a 90° pulse duration of 2 μs. The recycling time between two scans was 60 s. Spectra are referred to 1 M aqueous solution of LiCl, set at 0 ppm. T1 relaxation times were estimated by using variable recycling times, until full intensity of the line is observed. Decomposition of the spectra was achieved using the DMfit software [14].

Temperature-dependent electronic conductivity measurements were carried out with the four-probe technique [15], using a direct current. The temperature was decreased down to −100 °C, then progressively raised to 400 °C and again lowered to room temperature. Because of the low-temperature synthesis, the studied material could not be sintered. For this reason, pellets (8 mm of diameter and approximately 1.2 mm in thickness) were only obtained by compacting 200 mg of powder at 8 t/cm$^2$ under vacuum.

## 3. Results and discussion

### 3.1. Study of the starting materials at room temperature

#### 3.1.1. XRD analysis

The alkaline ions, present in the electrolyte during the electrochemical oxidation of cobalt oxide, are likely to play a determinant role on the final structure and composition of the synthesized material. The XRD patterns of the three parent materials that were respectively prepared in ternary electrolyte, in LiOH and in KOH, correspond to that of a $Co_3O_4$ type phase and can be indexed in the cubic space group $Fd_3/m$. The material, synthesized in ternary electrolyte, is monophasic, whereas the materials prepared in KOH or LiOH contain a secondary phase, as suggested by additional diffraction peaks. The results of Rietveld refinement of the X-ray powder diffraction pattern of the materials are presented in Figs. 1 and 2, and reported in the first line (RT-i) of Tables 1 and 2. (The data obtained for the material, synthesized in ternary electrolyte, were already reported in our previous paper and are not presented here [13]). For the $Co_3O_4$(KOH) parent material (RT-i diagram), data refinement leads to a $Co_3O_4$ spinel type phase, with lower than 1 wt% of a hexagonal CoOOH type phase, exhibiting the following hexagonal cell parameters $a_{\mathrm{hex.}} = 2.829(5)$ Å and $c_{\mathrm{hex.}} = 13.20(1)$ Å. The formation of such a phase is not surprising, because it is an intermediate phase, which appears before the formation of $Co_3O_4$, during the electrochemical oxidation of CoO [16]. The $Co_3O_4$(LiOH) parent material contains 80 wt% of a $Co_3O_4$ spinel type phase and 20 wt% of a $LiCoO_2$ type phase. The latter appears to be the high temperature variety, exhibiting an O3 oxygen packing, with the following hexagonal cell parameters $a_{\mathrm{hex.}} = 2.8224(6)$ Å and $c_{\mathrm{hex.}} = 14.044(5)$ Å.

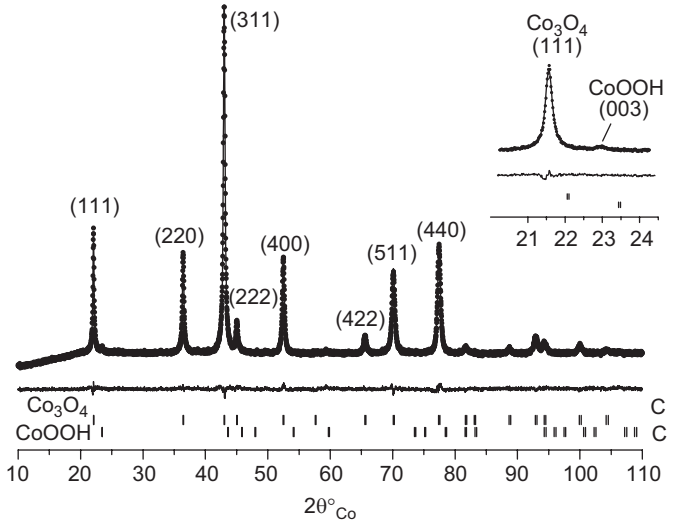


**Fig. 1.** Results of Rietveld refinement of the X-ray powder diffraction pattern of the $Co_3O_4$(KOH) material, prepared in KOH electrolyte. Observed and calculated profiles, peak positions and difference between observed and calculated profiles are represented here.

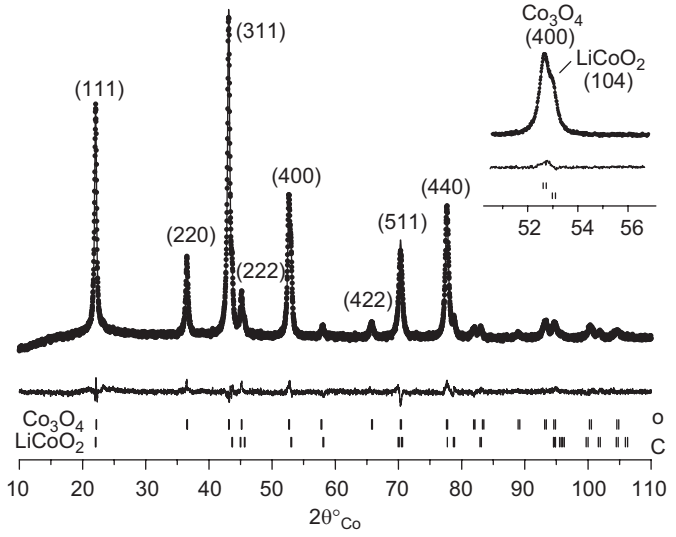


**Fig. 2.** Results of Rietveld refinement of the X-ray powder diffraction pattern of the $Co_3O_4$(LiOH) material, prepared in LiOH electrolyte. Observed and calculated profiles, peak positions and difference between observed and calculated profiles are represented here.

The three parent materials have slightly different cobalt occupancies in the tetrahedral sites (8*a*). Indeed, 82% of tetrahedral sites are occupied in the $Co_3O_4$(KOH) material (Table 1), 77% in $Co_3O_4$(ternary) [13] and only 66% in $Co_3O_4$(LiOH) (Table 2). These differences could be explained by the presence of different amounts of alkaline ions within the spinel structure.

### 3.1.2. Chemical analysis

Table 3 reports the weight percentages of cobalt and alkaline ions, as well as the average oxidation state of cobalt, and illustrates differences in material compositions, depending on the electrolyte. As soon as the electrolyte contains lithium ions, a significant amount of lithium is detected in the material, whereas it is not the case for potassium ions, which can be considered as negligible in $Co_3O_4$(KOH) and $Co_3O_4$(ternary). The values of cobalt oxidation state are higher than that expected in an ideal spinel $Co^{II}Co_2^{III}O_4$ (2.66) and confirm the presence of $Co^{4+}$, in particular in the "$Co_3O_4$(LiOH)" and "$Co_3O_4$(ternary)" materials, as suspected by XRD analysis. On the other hand, the hydrogen/cobalt ratio detected is close to 0.3 in the three materials.

XRD analysis (Rietveld refinement) has shown the presence of 20 wt% $LiCoO_2$ in the $Co_3O_4$(LiOH) material, corresponding to 1.42 wt% of Li in the mixture, which is lower than the amount of 2.12 wt%, detected by elemental analysis. This difference suggests that about 0.7 wt% of lithium ions (relative to the total mass of the mixture) are present within the spinel structure. This percentage is in full accordance with that found in the $Co_3O_4$(ternary) spinel phase, for which no $LiCoO_2$ was detected [13]. Corresponding to a lithium/cobalt ratio of 0.09, it is in agreement with the number of cobalt vacancies found in both spinel phases.

## 3.2. In situ XRD study of the thermal behavior

As reported previously, a thermal treatment of the $Co_3O_4$(ternary) material was shown to have a strong influence on the electric conductivity, in relation with the material composition. Keeping in mind that the composition is affected by the nature of the alkaline ions of the electrolyte, the effect of heat-treatment on the structure of the materials, prepared in the various electrolytes, was followed in-situ by XRD. The successive XRD patterns, collected with increasing temperature of the chamber until 700 °C, are presented in Fig. 3, in the case of $Co_3O_4$(KOH) and in Fig. 4, in the case of $Co_3O_4$(LiOH).

From a general point of view, the reduction of the width of the diffraction lines, observed during the experiment, can be attributed to an increasing crystallization of the materials. In addition, a shift of the diffraction lines towards the low angles during heating and

**Table 1**
Refinement parameters of the XRD patterns, obtained during in-situ analysis of the $Co_3O_4$(KOH) sample, prepared in KOH electrolyte.

| T° of data collection | $Co_3O_4$ type phase | | | | CdO type phase | |
|---|---|---|---|---|---|---|
| | $a_{cub.}$ | Oxygen position *u* | Cobalt occupancy | | wt% CdO | $a_{cub.}$ |
| | | | 8*a* sites | 16*d* sites | | |
| RT-i | 8.0972 (5) | 0.2611 (3) | 0.82 (2) | 0.96 (2) | – | – |
| 100 °C | 8.0979 (8) | 0.2613 (3) | 0.82 (2) | 0.96 (2) | – | – |
| 200 °C | 8.0924 (8) | 0.2610 (3) | 0.81 (2) | 0.97 (2) | – | – |
| 300 °C | 8.0993 (6) | 0.2613 (3) | 0.85 (2) | 0.96 (2) | – | – |
| 400 °C | 8.1102 (5) | 0.2619 (3) | 0.92 (2) | 1.00 (2) | 0.70 (5) | 4.725 (2) |
| 500 °C | 8.1212 (5) | 0.2627 (3) | 0.94 (2) | 0.99 (2) | 1.35 (7) | 4.7315 (6) |
| 600 °C | 8.1281 (5) | 0.2627 (4) | 0.92 (2) | 0.95 (2) | 2.7 (1) | 4.7387 (5) |
| 700 °C | 8.1451 (4) | 0.2616 (4) | 0.93 (2) | 0.95 (2) | 2.4 (1) | 4.7439 (4) |
| RT-f | 8.0813 (3) | 0.2630 (3) | 0.92 (2) | 0.96 (2) | 2.04 (7) | 4.6960 (4) |

**Table 2**
Refinement parameters of the XRD patterns, obtained during in-situ analysis of the $Co_3O_4$(LiOH) sample, prepared in LiOH electrolyte.

| T° of data collection | $Co_3O_4$ type phase | | | | $LiCoO_2$ type phase | | | |
|---|---|---|---|---|---|---|---|---|
| | $a_{cub.}$ | Oxygen position $u$ | Cobalt occupancy | | wt% $LiCoO_2$ | $a_{hex.}$ | $c_{hex.}$ | Oxygen position $z$ |
| | | | 8*a* sites | 16*d* sites | | | | |
| RT-i | 8.0761 (9) | 0.2628 (7) | 0.66 (2) | 0.94 (5) | 20.3 (1.6) | 2.8224 (6) | 14.044 (5) | 0.254 (3) |
| 100 °C | 8.079 (1) | 0.2628 (7) | 0.67 (2) | 0.95 (5) | 20.6 (0.5) | 2.8235 (7) | 14.07 (6) | 0.253 (3) |
| 200 °C | 8.073 (1) | 0.2630 (7) | 0.68 (2) | 0.97 (5) | 20.6 (0.6) | 2.8255 (8) | 14.09 (7) | 0.252 (3) |
| 300 °C | 8.0813 (9) | 0.2622 (6) | 0.70 (2) | 0.96 (4) | 19.5 (0.4) | 2.8278 (7) | 14.138 (6) | 0.254 (2) |
| 400 °C | 8.0978 (6) | 0.2624 (5) | 0.83 (2) | 0.96 (3) | 25.8 (0.9) | 2.8310 (4) | 14.163 (3) | 0.257 (1) |
| 500 °C | 8.1138 (4) | 0.2623 (4) | 0.91 (2) | 0.97 (3) | 27.4 (0.7) | 2.8344 (3) | 14.203 (2) | 0.258 (1) |
| 600 °C | 8.1262 (3) | 0.2619 (4) | 0.93 (2) | 0.95 (3) | 26.9 (0.7) | 2.8373 (2) | 14.2427 (8) | 0.2576 (8) |
| 700 °C | 8.1442 (2) | 0.2619 (5) | 0.95 (2) | 0.96 (4) | 24.9 (0.9) | 2.8422 (2) | 14.2885 (7) | 0.2559 (6) |
| 600 °C | 8.1263 (2) | 0.2626 (5) | 0.95 (2) | 0.95 (4) | 22.5 (0.7) | 2.8369 (1) | 14.2447 (6) | 0.2543 (6) |
| 400 °C | 8.1071 (2) | 0.2630 (4) | 0.95 (2) | 0.96 (4) | 23.1 (0.6) | 2.8289 (1) | 14.1799 (5) | 0.2543 (6) |
| 200 °C | 8.0918 (2) | 0.2626 (4) | 0.96 (2) | 0.96 (4) | 23.9 (0.6) | 2.8216 (1) | 14.1161 (6) | 0.2562 (5) |
| RT-f | 8.0815 (2) | 0.2613 (4) | 0.96 (2) | 0.96 (5) | 24.3 (0.3) | 2.8163 (1) | 14.0673 (5) | 0.2559 (6) |

**Table 3**
Weight percentages of cobalt, lithium, potassium, carbon and hydrogen elements, corresponding molar ratios and average oxidation state of cobalt, in the materials prepared in the different electrolytes.

| Material | wt% | | | | | Molar ratio | | | Average oxid. state of Co |
|---|---|---|---|---|---|---|---|---|---|
| | Co | Li | K | H | C | H/Co | Li/Co | K/Co | |
| $Co_3O_4$(KOH) | 68.6 | – | 0.24 | 0.4 | 0.7 | 0.34 | – | 0.01 | 2.68 |
| $Co_3O_4$(LiOH) | 63.5 | 2.12 | – | 0.4 | 1.5 | 0.37 | 0.28 | – | 2.72 |
| $Co_3O_4$(ternary) | 69.0 | 0.69 | 0.12 | 0.38 | 0.7 | 0.32 | 0.09 | 0.003 | 2.77 |

towards the high angles during cooling can be assigned to a modification of the cell parameters, due to thermal dilatation.

The thermal evolutions of the structural parameters, deduced from refinement of the XRD data, are gathered in Tables 1 and 2, for $Co_3O_4$(KOH) and $Co_3O_4$(LiOH), respectively.

In the case of $Co_3O_4$(KOH), beyond 400 °C, new peaks emerge in addition to those corresponding to the spinel phase. They can be attributed to a CdO type phase, which is suspected to be present in an amorphous form at the beginning and to crystallize during the experiment. Structural refinement concludes indeed to the presence of 2 wt% of CdO phase with a cubic cell parameter of 4.6960(4) Å. This phase could be formed after dissolution of cadmium from the negative electrode, migration within the KOH electrolyte and deposition under the CdO form at the positive electrode, where the $Co_3O_4$ phase is synthesized. Such a behavior is sometimes observed in very specific cycling conditions of Ni–Cd cells [17]. It should also be noticed that the CoOOH phase detected in the starting material cannot be characterized by Rietveld refinement all along the thermal study, because of its small amount (<1%); no mention of it is therefore made in Table 1. Nevertheless, an hexagonal phase in the same proportion is still detected on the RT-f diagram obtained at room temperature at the end of the experiment.

In the case of $Co_3O_4$(LiOH), the refinement results in Table 2 show that, beyond 400 °C, 5 wt% more of $LiCoO_2$ phase appear in addition to the 20% that are already present, which suggests the presence of lithium ions in the spinel type phase, until this temperature at least. This behavior is quite similar to that observed for the material synthesized in ternary electrolyte, which led to crystallization of 8 wt% of a $LiCoO_2$ phase after thermal treatment [13]. On the basis of the chemical analysis, the materials $Co_3O_4$(LiOH) (mixture of lithiated $Co_3O_4$ and $LiCoO_2$) and $Co_3O_4$(ternary) (lithiated $Co_3O_4$ only) present 0.7 wt% of lithium (relative to the total mass of the sample) in their spinel structures. The lithium amount released from the spinel during heat-treatment, to form 5 and 8 wt% of $LiCoO_2$, respectively, corresponds to 0.35 and 0.56 wt%. It seems therefore that all lithium ions are not released into $LiCoO_2$, but minor quantities (0.35 and 0.14 wt%) are still present in the spinel structures, even after the heat-treatment.

Let us now consider and compare the thermal evolutions of the $Co_3O_4$ type phases, depending on the electrolyte nature. First, as suggested by comparison of Tables 1 and 2, cobalt occupancies in tetrahedral and octahedral sites seem to follow similar behavior for all the materials: when temperature increases, especially beyond 350 °C, cobalt occupancy in the tetrahedral sites tends to increase (it reaches 92% for $Co_3O_4$(KOH) and 96% for $Co_3O_4$(LiOH), at the end of the experiment), while cobalt occupancy in the octahedral sites remains stable, around 94–96%. At the very end of the experiment (after cooling down to room temperature), the three materials synthesized in KOH, LiOH or ternary electrolyte tend to a spinel structure, with similar cobalt occupancy and with a formula close to $Co_{0.96}[Co_{1.92}]O_4$.

Fig. 5 allows us to compare the thermal evolution of the cubic cell parameters of the spinel phases that are present within the three samples studied. The initial cell parameters are different. As the cell parameter in spinel structure is conditioned by the octahedral site size, different $Co^{4+}$ ions amounts can be assumed within the three parent materials. On the other hand, the variations of the cell parameters as a function of temperature exhibit strong similarities, whatever the electrolyte. At the end of the experiment, the cell parameters tend to be equal to the same value, 8.081 Å at room temperature, which is in accordance with the formation of a spinel phase $Co_{0.96}[Co_{1.92}]O_4$ , whatever the electrolyte used for the synthesis. The general shape of the curves shows a decrease of the cubic parameter, followed by an increase. In order to explain this behavior, the variations of the cell parameters upon heating and cooling of the two phases ($Co_3O_4$ and $LiCoO_2$), which are present in the $Co_3O_4$(LiOH) sample, are compared in Fig. 6. The cell parameters of the hexagonal $LiCoO_2$ type phase exhibit a quasi-linear increase with temperature, in good accordance with thermal dilatation, while the cell parameter of the cubic $Co_3O_4$ type phase shows a peculiar variation from RT to 500 °C. During the cooling, there is no change in cationic distribution in the spinel structure, while the peculiar behavior during the heating, between RT and 500 °C, can be related to the increasing occupancy of the tetrahedral sites by cobalt ions. The $H_2O$ departure, which occurs during heat-treatment, entails an increase of the Co/O atomic ratio and of the cobalt occupancy in

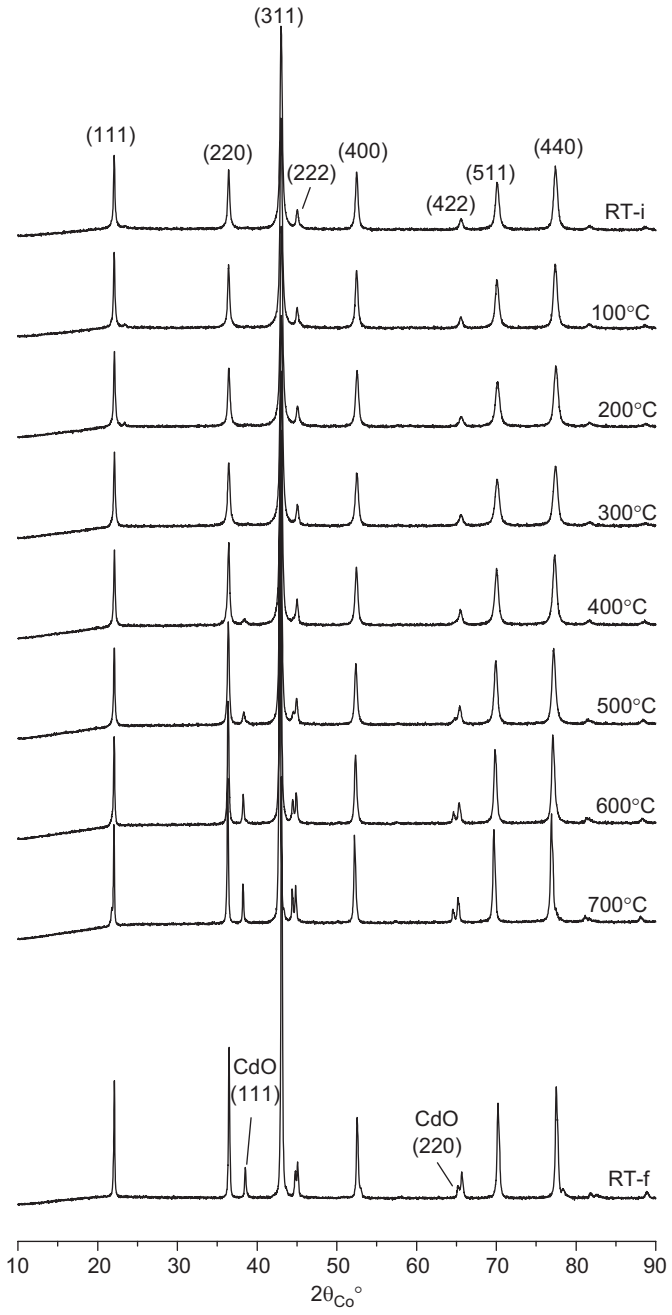


**Fig. 3.** Thermal evolution of the X-ray diffraction patterns of the $Co_3O_4$(KOH) material, prepared in KOH electrolyte. The sample was placed inside a high temperature chamber, connected to the diffractometer.

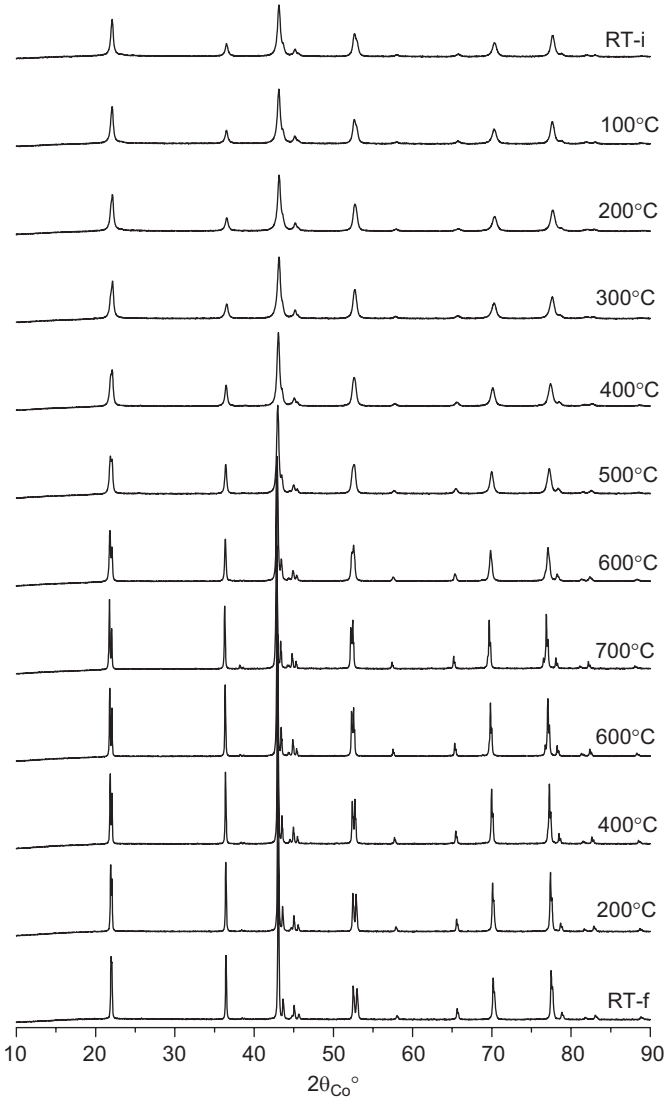


**Fig. 4.** Thermal evolution of the X-ray diffraction patterns of the $Co_3O_4$(LiOH) material, prepared in LiOH electrolyte. The sample was placed inside a high temperature chamber, connected to the diffractometer

tetrahedral sites in the spinel structure. The resulting cationic redistribution leads to an increase of the $Co^{4+}$ amount in the octahedra framework, and consequently to a decrease of the $a_{cub.}$ parameter. Fig. 5 suggests that the formation of $Co^{4+}$ ions with increasing temperature in the 200–500 °C range is not restricted to lithium containing materials, but occurs whatever the electrolyte nature.

### 3.3. Thermal analysis

TGA analysis was performed on the three starting samples. Fig. 7 compares weight lost by each material during heating. All the curves exhibit similar behavior. A first weight loss is detected

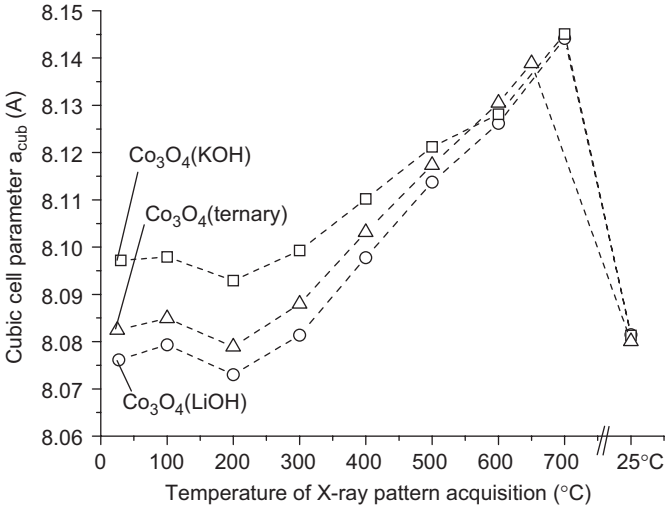


**Fig. 5.** Comparison of the thermal evolutions of the cell parameters of the $Co_3O_4$(KOH), $Co_3O_4$(LiOH) and $Co_3O_4$(ternary) materials, synthesized in different electrolytes.

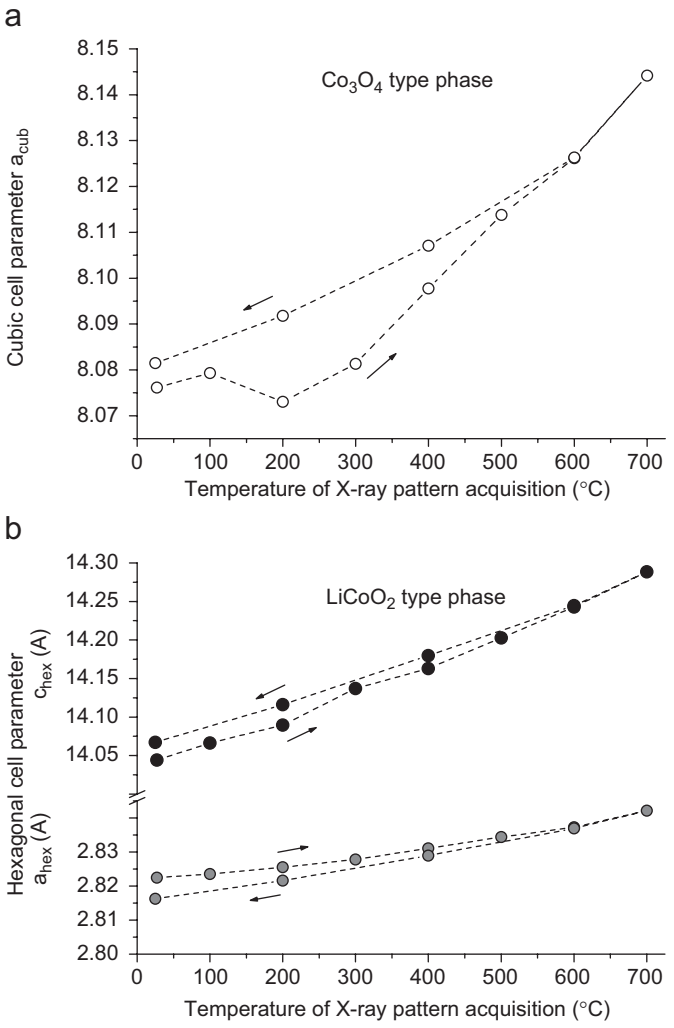


**Fig. 6.** Variations: (a) of the cubic cell parameter of the spinel $Co_3O_4$ type phase and (b) of the hexagonal cell parameters of the $LiCoO_2$ type phase, when the $Co_3O_4$(LiOH) material, synthesized in LiOH electrolyte, is heated inside a variable temperature chamber, connected to the diffractometer. The parameters were determined thanks to refinement of the X-ray data.

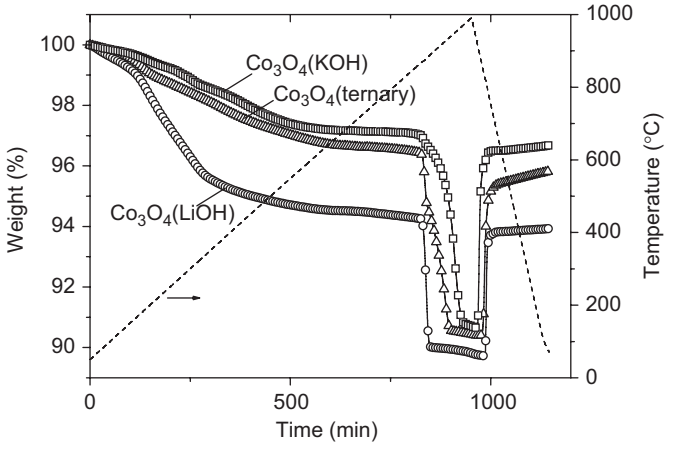


**Fig. 7.** Thermogravimetric analysis curves of the (□) $Co_3O_4$(KOH), (○) $Co_3O_4$(LiOH) and (△) $Co_3O_4$(ternary) materials, prepared in different electrolytes.

between room temperature and 850 °C. In our previous work [13], mass spectroscopy analysis, performed under argon flux, had emphasized a quasi-continuous departure of gaseous $H_2O$ in the RT-700 °C range, for the $Co_3O_4$(ternary) material [13]. The $H_2O$ removal was attributed, until 100 °C, to a release of water adsorbed on the material surface, and beyond 100 °C, to decomposition of hydroxyls groups within the structure. A small amount of $CO_2$, assigned to adsorbed gas on the material surface, was observed simultaneously with the $H_2O$ departure. It should be noticed that the weight loss observed for the $Co_3O_4$(LiOH) material is significantly higher than those detected for the other two materials. This difference may be associated with the higher amount of carbon titrated in the $Co_3O_4$(LiOH) sample. Carbon excess should come from a $Li_2CO_3$ type phase, as we will see in the NMR section.

**Table 4**
Weight losses observed during thermogravimetric analysis of the $Co_3O_4$(KOH), $Co_3O_4$(LiOH) and $Co_3O_4$(ternary) materials, prepared in different electrolytes.

| Materials | Weight loss (%) | |
|---|---|---|
| | RT−850 °C range | 850–1000 °C range |
| $Co_3O_4$(KOH) | 3.05 | 6.63 |
| $Co_3O_4$(LiOH) | 6.05 | 4.79 |
| $Co_3O_4$(ternary) | 3.58 | 6.41 |

Strong and reversible weight losses are observed beyond 850 °C. Table 4 summarizes weight losses, observed for the three studied samples. The weight losses observed during the decomposition of the $Co_3O_4$(KOH) and $Co_3O_4$(ternary) materials, which are constituted of a quasi pure spinel phase, are similar and coherent with the theoretical value of 6.64%, which is expected for the decomposition of $Co_3O_4$ into CoO. In the case of the $Co_3O_4$(LiOH) sample, the lower value (4.79%) results from the presence, in addition to $Co_3O_4$, of 20 wt% of $LiCoO_2$ phase, which remains unchanged.

### 3.4. Electrical properties

As reported in the experimental section, the conductivity measurements were performed with the four probes technique [15], using ion-blocking electrodes and measuring the current intensity in a stationary regime so that any ionic contribution (of the lithium ions) to the conductivity can be neglected.

In the investigation of the role of the electrolyte, the influence of temperature on the electronic conductivity of the materials, synthesized in different electrolytes, was studied in the −100 to 400 °C range. As shown in Fig. 8, the $Co_3O_4$(LiOH) and $Co_3O_4$ (ternary) materials exhibit, at room temperature, higher conductivity than $Co_3O_4$(KOH). This difference can be related to the values of cobalt oxidation state for each material (Table 3). Indeed, in the $Co_3O_4$(LiOH) and $Co_3O_4$(ternary) materials, the presence of $Co^{4+}$ in the $[Co_2O_4]$ framework induces a local electronic delocalization in the $T_{2g}$ band of cobalt and leads to an increase of conductivity, as compared to classical $Co_3O_4$. As demonstrated in a previous paper [12], this behavior is restricted at a local scale, due the small amount of $Co^{4+}$ ions and the presence of defects in the spinel structure, explaining why electronic conductivities are still thermally activated. Moreover, as the experiment is performed on compressed pellets (not sintered), the grain boundaries can also contribute to the activation energy. On the opposite, in the $Co_3O_4$(KOH) material, which exhibits a value of oxidation state close to that of ideal $CoCo_2O_4$, the amount of $Co^{4+}$ ions is very small. With only $Co^{3+}$ in the edge-sharing octahedra sublattice, the $T_{2g}$ band is fully filled, leading to a semi-conductor behavior. The initial electronic conductivities that are observed for the three studied materials are in good agreement with the difference of

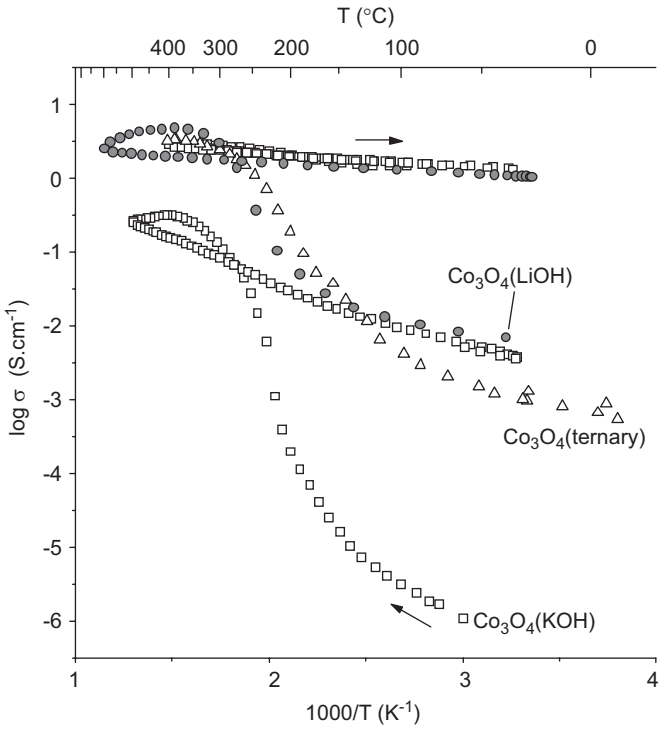


**Fig. 8.** Variation of electrical conductivity logarithm versus reciprocal temperature, for the three materials, prepared in different electrolytes.

cell parameters, presented in the "XRD" section and related to the amount of $Co^{4+}$ ions. Indeed, $Co_3O_4$(LiOH), which exhibits the lowest cubic cell parameter, presents the highest conductivity, and $Co_3O_4$(KOH), which has the highest cubic cell parameter, presents the lowest conductivity.

The increase of temperature entails the same behavior for the three samples: their electronic conductivities increase in an irreversible way, after a heat treatment up to 400 °C. It has been established that this jump in electronic conductivity is associated to an increase of the $Co^{4+}/Co^{3+}$ ratio, resulting from the cobalt cationic redistribution [13]. With a higher amount of $Co^{4+}$ and a lower quantity of defects, such as hydrogen and lithium, electronic delocalization is no more limited at the local scale and can be extended. Above 400 °C, the electronic conductivity decreases slowly; we can consider that, at too high temperature, the amount of $Co^{4+}$ ions decreases slowly. This behavior can be explained by the formation of a $LiCoO_2$ phase, which tends to decrease slowly the average oxidation state of cobalt in the spinel phase.

### 3.5. $^7$Li NMR study

The HT-$LiCoO_2$ phase represents 20 wt% in the $Co_3O_4$(LiOH) material and grows up during the heat-treatment. In order to investigate the possible contribution of this $LiCoO_2$ phase to the high conductivity of the material, $^7$Li NMR study was performed on the sample synthesized in LiOH. Moreover, to obtain more information on materials changes during temperature increasing, $Co_3O_4$(LiOH) was heated at 400 and 650 °C under argon atmosphere, leading to materials that are denoted as $Co_3O_4$(LiOH)-400 and $Co_3O_4$(LiOH)-650, which were also studied by NMR. The NMR investigation of samples, synthesized in ternary electrolyte, has been previously reported [13]. To summarize, this study has allowed to demonstrate that (i) changes occur in the spinel structure (different sites of lithium and/or different oxidation states of cobalt), (ii) a LiOH type phase is formed during heat-treatment and (iii) the lithium cobaltite phase that grows during heat-treatment is the $Li_{1.0}CoO_2$ insulating stoichiometric phase.

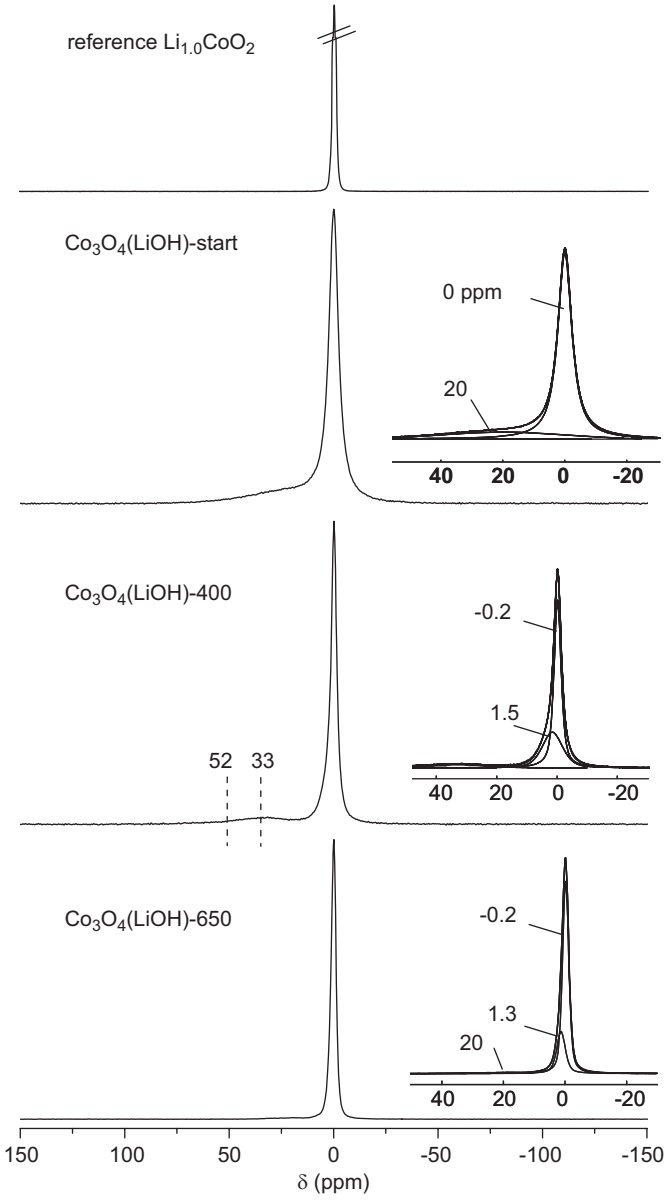


**Fig. 9.** $^7$Li MAS NMR spectra of the $Co_3O_4$(LiOH) samples—starting material, then ex situ heat-treated at 400 and 650 °C—in comparison with stoichiometric $Li_{1.0}CoO_2$, obtained by classical solid-state reaction.

The spectra of the $Co_3O_4$(LiOH) starting material and of the $Co_3O_4$(LiOH)-400 and $Co_3O_4$(LiOH)-650 heat-treated samples are presented in Fig. 9. It can be compared with that of reference stoichiometric $Li_{1.0}CoO_2$.

In the $Co_3O_4$(LiOH) starting material, two different signals at 0 and 20 ppm are observed. The 0 ppm signal is assigned to an overlap of lines, attributed to $LiCoO_2$ (−0.5 ppm) and $Li_2CO_3$ (~0 ppm) [13], while the narrow signal at 20 ppm is attributed to lithium in the spinel structure [12]. The shape of the 0 ppm NMR signal does not allow an unambiguous decomposition into $Li_2CO_3$ and $LiCoO_2$ components. However, as $Li_2CO_3$ is not observed by XRD, one can consider that it represents a minor amount. Indeed, in the hypothesis of an absence of $Li_2CO_3$, comparison of signal

**Table 5**
Comparison of the NMR shifts, observed for the $Co_3O_4$(LiOH) and $Co_3O_4$(ternary) [13] materials—starting and heat-treated samples.

| NMR shifts $\delta$ (ppm) | | | | | | | | |
|---|---|---|---|---|---|---|---|---|
| Sample | | $Li_xCo_3O_4$ | | | Unknown | LiOH | $Li_2CO_3$ | $LiCoO_2$ |
| $Co_3O_4$(ternary) [13] | Start | | | 22 | 6.3 | | 0.1 | |
| | 370 | 52 | 34 | | 6.3 | | 0.1 | |
| | 650 | | | 22 | 6.3 | 1.3 | | 0 |
| $Co_3O_4$(LiOH) | Start | | | 19 | | | | 0 |
| | 400 | 52 | 33 | | | 1.5 | | −0.2 |
| | 700 | | | 19 | | 1.3 | | −0.2 |

magnitudes indicates that the 0 ppm signal would correspond to around 72% of the lithium atoms. The total lithium amount detected in the material from chemical analysis is 2.1 wt% (Table 3), which would then lead to 21 wt% of $LiCoO_2$ phase, in agreement with the XRD results. Besides, the T1 relaxation time of the 0 ppm signal is higher than 4 s, which excludes the possibility of a $Li_xCoO_2$ phase with a lithium content in the $0.94 < x < 1$ range, containing localized $Co^{4+}$ ions [18]. Indeed, the relaxation time of the NMR signal is very sensitive to the presence of paramagnetic species, which shorten it drastically. So, lithium cobaltite phase is the stoichiometric $Li_{1.0}CoO_2$ phase, as previously observed by Tronel et al. [12].

The spectrum of the $Co_3O_4$(LiOH)-400 heat-treated sample exhibits four different signals: a signal (50% of lithium atoms in material) around −0.2 ppm, related to the $Li_{1.0}CoO_2$ phase (probably still mixed with a small amount of $Li_2CO_3$), a new signal at 1.5 ppm (40% of lithium), and two secondary signals (10% of lithium) at 33 and 52 ppm. On the spectrum of the $Co_3O_4$ (LiOH)-650 sample, the two signals at 33 and 52 ppm shift again to 20 ppm, whereas the two signals at 0 and 1.5 ppm are unchanged. A similar behavior was observed in samples synthesized in ternary electrolyte [13].

The NMR shifts observed for each sample, synthesized in LiOH electrolyte, are reported in Table 5 and compared to those obtained for the samples, synthesized in ternary electrolyte. Therefore, the 1.5 ppm signal can be assigned to a LiOH type phase, which appears beyond 400 °C. The signals detected at 20, 33 and 52 ppm can be assigned to lithium, with different surroundings in the spinel structure. Once again, NMR measurements highlight changes occurring within the spinel phase, with increasing temperature. The 6.3 ppm signal observed in the material series, synthesized in ternary electrolyte, and not clearly explained, does not appear in the present material series, maybe because of a larger magnitude of the $LiCoO_2$ signal next to it.

## 4. Conclusion

The results, reported in our previous paper for a $Co_3O_4$ type material, obtained by electrochemical synthesis in ternary electrolyte (LiOH–NaOH–KOH), can be extended to other electrolytes. Depending on the nature of the electrolyte, the amounts of $H^+$ and $Li^+$ ions in spinel framework can be monitored. Cobalt vacancies, either in tetrahedral or in octahedral sites, are present for all the materials. The electronic conductivity is directly related to the amount of $Co^{4+}$ ions in the octahedral sites, which lead to electronic delocalization. During the thermal treatment of the material, $H_2O$ is extracted from the spinel structure, while a part of lithium is removed via the $LiCoO_2$ formation. These reactions entail a structural reorganization, which leads to an increase of the amount of divalent cobalt ions in tetrahedral sites and of the $Co^{4+}/Co^{3+}$ ratio in the octahedral framework. As a result, the electronic conductivity of the spinel phase is strongly increased by the thermal treatment.

## Acknowledgments

The authors wish to thank C. Denage and P. Dagault for technical assistance, E. Lebraud and S. Pechev for X-ray diffraction and R. Decourt for electric properties measurements. SAFT, ANRT and Region Aquitaine are acknowledged for their financial support.

## References

[1] M. Oshitani, H. Yufu, K. Takashima, S. Tsuji, Y. Matsumaru, J. Electrochem. Soc. 136 (6) (1989) 1590–1593.
[2] M. Oshitani, M. Watada, T. Tanaka, T. Iida, in: The Electrochemical Society Proceedings Series, Pennington, NJ, 1994, p. 303.
[3] P. Benson, G.W.D. Briggs, W.F.K. Wynne-Jones, Electrochim. Acta 9 (1964) 281–288.
[4] M. Butel, L. Gautier, C. Delmas, Solid State Ionics 122 (1999) 271–284.
[5] V. Pralong, A. Delahaye-Vidal, B. Beaudoin, J.B. Leriche, J.M. Tarascon, J. Electrochem. Soc. 147 (4) (2000) 1306.
[6] V. Pralong, A. Delahaye Vidal, B. Beaudoin, J.B. Leriche, J. Scoyer, J.M. Tarascon, J. Electrochem. Soc. 147 (6) (2000) 2096–2103.
[7] T. Tanaka, J. Imaizumi, T. Iida, JP200152695, 2001.
[8] A. Yamawaki, S. Nakahori, T. Hamamatsu, Y. Baba, EP 0757395[a]1, 1997.
[9] F. Kato, F. Tanigawa, Y. Dansui, K. Yuasa, EP 0851516[a]2, 1998.
[10] Y. Furukawa Denchi, JP 330858, 1995.
[11] K. Yuasa, JP 2003031216, 2003.
[12] F. Tronel, L. Guerlou-Demourgues, M. Ménétrier, L. Croguennec, L. Goubault, P. Bernard, C. Delmas, Chem. Mater. 18 (25) (2006) 5840–5851.
[13] M. Douin, L. Guerlou-Demourgues, M. Ménétrier, E. Bekaert, L. Goubault, P. Bernard, C. Delmas, Chem. Mater. 20 (2008) 6880–6888.
[14] D. Massiot, F. Fayon, M. Capron, I. King, S. Le Calve, B. Alonso, J.-O. Durand, B. Bujoli, Z. Gan, G. Hoatson, Magn. Reson. Chem. 40 (1) (2002) 70–76.
[15] J. Laplume, L'onde électrique 335 (1955) 113–125.
[16] F. Tronel, L. Guerlou-Demourgues, M. Basterreix, C. Denage, L. Goubault, P. Bernard, C. Delmas, J. Power Sources 179 (2008) 837–847.
[17] SAFT, Private communication, 2008.
[18] M. Ménétrier, I. Saadoune, S. Levasseur, C. Delmas, J. Mater. Chem. 9 (1999) 1135.